

**The structure, composition, and application of the cell envelope from
*Caulobacter crescentus***

by

Michael D Jones

B. Science, Specialization in Biotechnology, University of Alberta, 2006

M. Science, Pharmaceutical Sciences, University of Alberta, 2008

A THESIS SUBMITTED IN PARTIAL FULFILLMENT
OF THE REQUIREMENTS FOR THE DEGREE OF

Doctor of Philosophy

in

THE FACULTY OF SCIENCE

(Microbiology and Immunology)

The University Of British Columbia

(Vancouver)

April 2015

© Michael D Jones, 2015

Abstract

This document provides brief instructions for using the `ubcdiss` class to write a -conformant dissertation in \LaTeX . This document is itself written using the `ubcdiss` class and is intended to serve as an example of writing a dissertation in \LaTeX . This document has embedded `()` and is intended to be viewed using a computer-based `()` reader.

Note: Abstracts should generally try to avoid using acronyms.

Note: at , both the `()` Ph.D. defence programme and the Library's online submission system restricts abstracts to 350 words.

Preface

At , a preface may be required. Be sure to check the guidelines as they may have specific content to be included.

Table of Contents

Abstract	ii
Preface	iii
Table of Contents	iv
List of Tables	vi
List of Figures	vii
List of Abbreviations	viii
0.1 General abbreviations	ix
0.2 Sugar abbreviations	x
Acknowledgments	xi
1 The core and O-polysaccharide structure of the <i>Caulobacter crescentus</i> lipopolysaccharide	1
1.1 Introduction	1
1.2 Results	2
1.2.1 Characterisation of whole LPS	2
1.2.2 Initial assessment and component analysis	2
1.2.3 O-Antigen structure determination (PS1)	3
1.2.4 Minor component determination	6
1.2.5 Rhamnan polysaccharide determination (PS2)	7
1.2.6 Core oligosaccharide determination	7
1.3 Methods	8
1.3.1 Bacterial strain construction and growth conditions	8
1.3.2 LPS isolation	9
1.3.3 Bligh Dyer Extraction	10
1.3.4 Gel electrophoresis	11
1.3.5 NMR spectroscopy	11
1.3.6 LPS Chromatography	11

1.3.7	Monosaccharide analysis	11
1.3.8	Determination of absolute configurations of monosaccharides	12
1.3.9	Methylation analysis	12
1.3.10	Periodate oxidation	12
1.4	Discussion	12
Bibliography		18
A Supporting Materials		21

List of Tables

Table 1.1	Nuclear magnetic resonance spectroscopy (NMR) data for <i>C. crescentus</i> polysaccharide (PS)1 (40°C) and deacylated PS1 (50°C). Me at 3.62/61.3 ppm.	15
Table 1.2	NMR data for the minor components of the double oxidized non-deacylated PS	16
Table 1.3	NMR data for <i>C. crescentus</i> PS2 and its NaIO ₄ oxidation product oligosaccharide (OS)1	17
Table 1.4	NMR data for the core oligosaccharide	17

List of Figures

Figure 1.1	Matrix assisted laser desorption/ionization-time of flight mass spectroscopy (MALDI-TOF) analysis of intact, whole lipopolysaccharide (LPS) from <i>C. crescentus</i>	2
Figure 1.2	¹ H nuclear magnetic resonance spectroscopy (NMR) spectra of <i>C. crescentus</i> O-specific polysaccharide (OPS)	4
Figure 1.3	The structure of the <i>C. crescentus</i> OPS.	5
Figure 1.4	2D NMR of <i>C. crescentus</i> polysaccharide (PS)1.	6
Figure 1.5	The structure of minor component, the end caps of the OPS.	7
Figure 1.6	The structure of the <i>C. crescentus</i> rhamnan.	8
Figure 1.7	The structure of the <i>C. crescentus</i> core oligosaccharide (OS).	9
Figure 1.8	Fragment of ¹ H- ¹³ C heteronuclear single quantum coherence (HSQC) spectrum of the core.	10

List of Abbreviations

0.1 General abbreviations

ABC	ATP-binding cassette
EDTA	Ethylenediaminetetraacetic acid
EPS	Extracellular polysaccharide
ESI	Electrospray ionization
GC-MS	Gas chromatography-mass spectroscopy
gCOSY	Gradient correlation spectroscopy
gHMBC	Gradient heteronuclear multiple bond coherence
gHSQC	Gradient heteronuclear single quantum coherence
HMBC	Heteronuclear multiple bond coherence
HMQC	Heteronuclear multiple-quantum correlation spectroscopy
HSQC	Heteronuclear single quantum coherence
LPS	Lipopolysaccharide
MALDI-TOF	Matrix assisted laser desorption/ionization-time of flight mass spectroscopy
NMR	Nuclear magnetic resonance spectroscopy
NOE	Nuclear Overhauser effect
NOESY	Nuclear Overhauser effect spectroscopy
OPS	O-specific polysaccharide
OS	Oligosaccharide
PBS	Phosphate-buffered saline
PS	Polysaccharide
S-layer	Protein surface layer
SDS-PAGE	Sodium dodecyl sulfate-polyacrylamide gel electrophoresis
TFA	Trifluoroacetic acid
TLC	Thin-layer chromatography
TCOSY	Total correlation spectroscopy
UV	Ultraviolet Light

0.2 Sugar abbreviations

Acknowledgments

Thank those people who helped you.

Don't forget your parents or loved ones.

You may wish to acknowledge your funding sources.

Chapter 1

The core and O-polysaccharide structure of the *Caulobacter crescentus* lipopolysaccharide

1.1 Introduction

Caulobacter crescentus is an aquatic alphaproteobacterium well known for a stalked, crescent cell morphology, asymmetric cell division, and a protein surface layer (S-layer). *C. crescentus* is a widely studied model organism for cell development and differentiation; despite this, the structure of its lipopolysaccharide (LPS) has not previously been fully determined.

Interest in the LPS of *C. crescentus* is focused on its immunological profile⁵ and its structural role as an anchor for the self-assembled, paracrystalline S-layer.⁶ The LPS of *C. crescentus* possesses a much reduced immunogenic activity, most likely due to its lipid A structure, which is significantly different from that of LPS from enteric bacteria. The lipid A structure has been reported⁵, it is a unique molecule containing a di-diaminoglucose backbone (instead of di-glucosamine) and two galacturonate moieties that replace the canonical phosphates that are on each end of the disaccharide in most lipid A molecules. The *C. crescentus* S-layer non-covalently attaches to the O-specific polysaccharide (OPS).⁶ However, the OPS structure has not been resolved. Genetic analyses have pointed towards the unusual N-acetylperosamine being a major component.⁷ A notable feature of this O-antigen is that it exists completely hidden beneath the S-layer, presumably inaccessible to the environment.⁶ Carbohydrate structures from non-pathogenic bacterial LPS are rarely studied and an LPS that is sequestered beneath an S-layer is not represented in the literature.

In the present study our data has determined the core oligosaccharide structure from *C. crescentus* CB15 NA1000, (advancing an earlier report of core composition⁸) as well as the central backbone and non-reducing ends of its OPS. Unexpectedly, we identified a previously unknown rhamnan polysaccharide. Along with previous reports on lipid A⁵ and extracellular polysaccharide (EPS),⁹ we believe that all the major carbohydrate structures in *C. crescentus* cell envelope have now been solved.

⁵John Smit et al. *Innate Immun*, **14**: 25–36, 2008.

⁶Stephen G Walker et al. *J Bacteriol*, **176**: 6312–6323, 1994.

⁷P. Awram and J. Smit. *Microbiology*, **147**: 1451–60, 2001.

⁸N. Ravenscroft et al. *J Bacteriol*, **174**: 7595–605, 1992.

⁹N. Ravenscroft et al. *J Bacteriol*, **173**: 5677–84, 1991.

1.2 Results

1.2.1 Characterisation of whole LPS

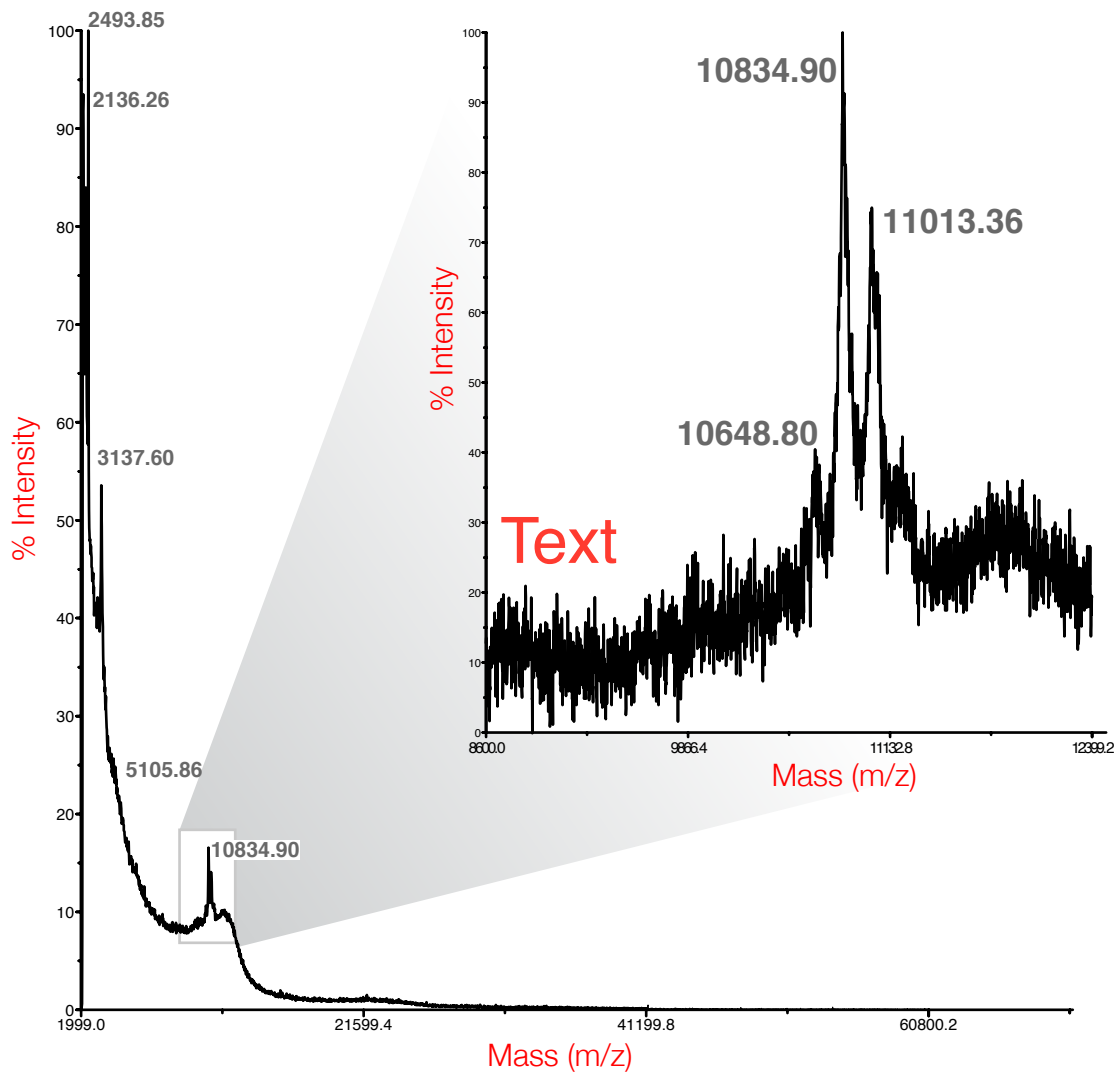


Figure 1.1: MALDI-TOF analysis of intact, whole LPS from *C. crescentus*. The insert highlights the peaks attributed to LPS. The major LPS peak is labelled 10834.90 m/z

1.2.2 Initial assessment and component analysis

The polysaccharide (PS) was released from the LPS by hydrolysis with acetic acid. ^1H nuclear magnetic resonance spectroscopy (NMR) spectrum of the PS (fig. 1.2)) contained a large number of partially overlapping signals of various intensities in the anomeric region. It was obviously not a regular polymer with well-defined repeating units. Attempts to separate this material by anion-exchange chromatography led

to the isolation of a number of fractions from neutral to slightly retained, but all of them had virtually identical NMR spectra. Methylation of the polysaccharide led to the identification of 3- and 3,4-substituted mannopyranose, terminal glucopyranose (derived from side-chain 3-O-methyl-glucose), terminal, 3-, 4-, and 2,4-substituted rhamnopyranose, 3-substituted Rha4NAc, and an unidentified derivative resembling methylated Rha4N that eluted between dimethylhexose derivatives and 3-substituted Rha4NAc. To identify the position of the methyl groups in naturally methylated monosaccharides, methylation was conducted with CD₃I. This confirmed the identification of tetramethylglucitol as originating from 3-O-methyl-glucose, but did not identify any other naturally methylated monosaccharides, visible in NMR spectra. An unknown derivative received two deuterated methyl groups.

1.2.3 O-Antigen structure determination (PS1)

A set of 2D spectra [gradient correlation spectroscopy (gCOSY), total correlation spectroscopy (TCOSY), nuclear Overhauser effect spectroscopy (NOESY), ¹H-¹³C gradient heteronuclear single quantum coherence (gHSQC), gradient heteronuclear multiple bond coherence (gHMBC)] was obtained for the PS. There were many (more than 20) lines of correlations from the anomeric signals. Later, after the analysis of PS degradation products, most of them could be assigned to particular structures (figs. 1.3, 1.5, and 1.6). Polysaccharide heterogeneity was not caused by random acetylation, but PS contained 4 methyl groups (one major and 3 minor). Monosaccharide analysis revealed L-Rha, D-Man, D-Rha4N (perosamine), and 3-O-methyl-D-glucose. Other methylated monosaccharides were not identified by GC-MS as alditol acetates, possibly due to low content or degradation during hydrolysis.

In an attempt to simplify the structure, PS was oxidized with NaIO₄, reduced with NaBD₄, hydrolyzed with 2% AcOH, and the products were separated on a Biogel P6 column to give a polymer and an oligosaccharide (OS), OS1. Analysis of OS1 will be described below. For some reason not all of the rhamnan was oxidized, and some of its signals persisted in the spectra of the remaining polymer (without side-chain Rha F). To remove the rest of it, the oxidation was repeated to produce PS1. Spectra still contained some signals of minor components, analyzed later. Assignment of the spectra of the non-oxidizable polymer PS1 was difficult due to complete or partial overlap of the H-2,3,4,5 signals of Rha4NAc. To improve signal spread, PS1 was deacetylated with 4 M NaOH. At this point the major polymer became positively charged and an attempt was made to separate it from the minor components using cation-exchange chromatography. However, all material was eluted together at high salt concentration, thus indicating that all components were chemically bound together. Assignment of the spectra (fig. 1.4, table 1.1) became possible at this stage due to better signal spread (H-4 signals of Rha4N moved to high field due to deacetylation) and the sequence shown on fig. 1.3 was proposed. Spectra contained the signals of two β-mannopyranose, 3-O-Me-α-Glcp, and two -Rhap4N. The following interresidual nuclear Overhauser effect (NOE) and heteronuclear multiple bond coherence (HMBC) correlations were used to determine the sequence: R1:L3, L1:Z3, Z1:Q3, Q1:W3, W1:X3, A1:X4. PS1 had trisaccharide repeating units composed of β-mannose and two α-Rha4NAc residues, and every second repeating unit carried a side branch of 3-O-Me-Glc. It seems that side-chains were present quite regularly at each second trisaccharide repeat of the main chain, because NOE correlations

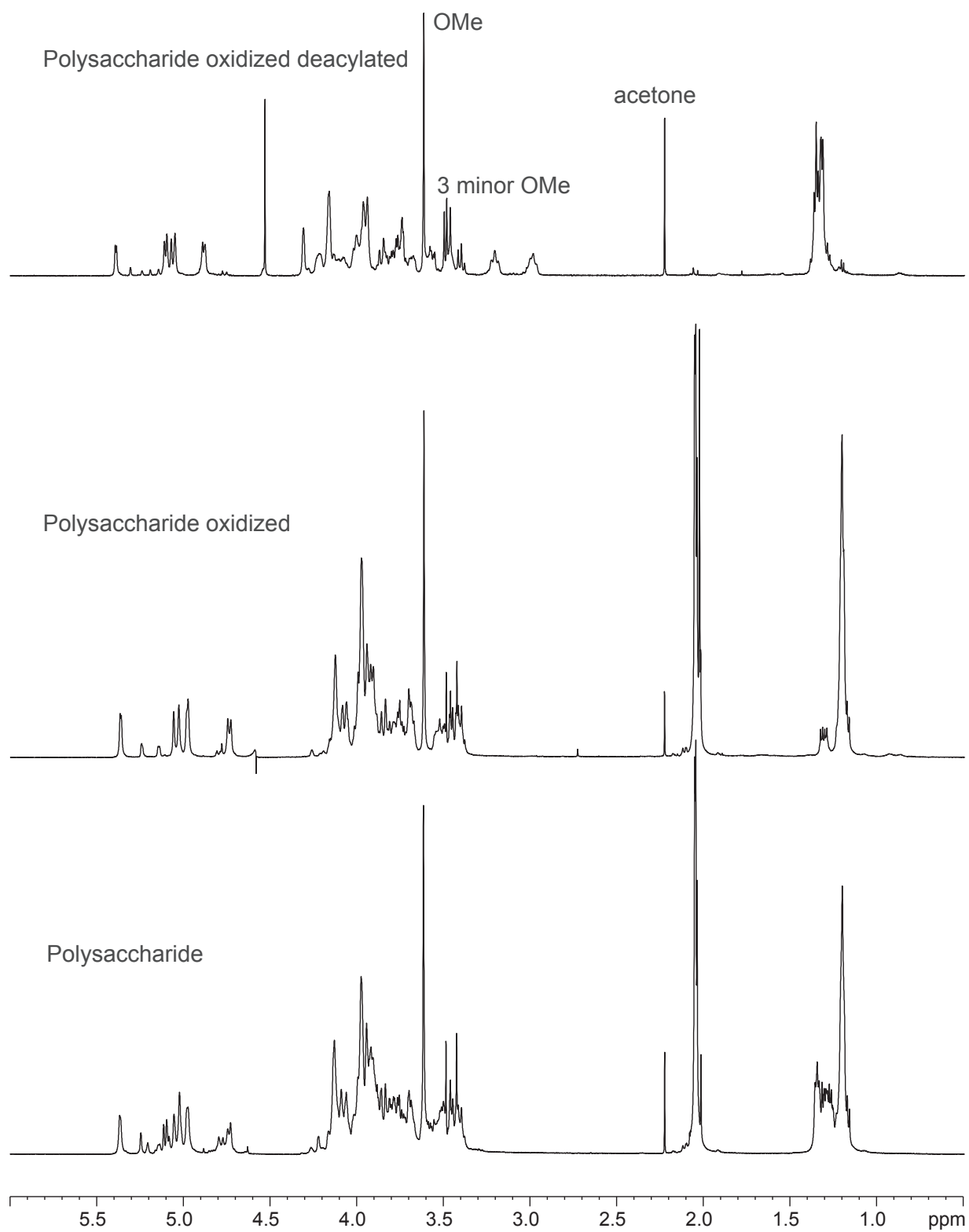


Figure 1.2: ^1H NMR spectra of the intact *C. crescentus* OPS (bottom trace), double oxidized polysaccharide (middle trace) and N-deacylated double oxidized polysaccharide (upper trace).

were observed between the repeating units with and without 3-OMe-Glc, and not between units of the same structure. Thus altogether, the repeating unit contained seven monosaccharides.

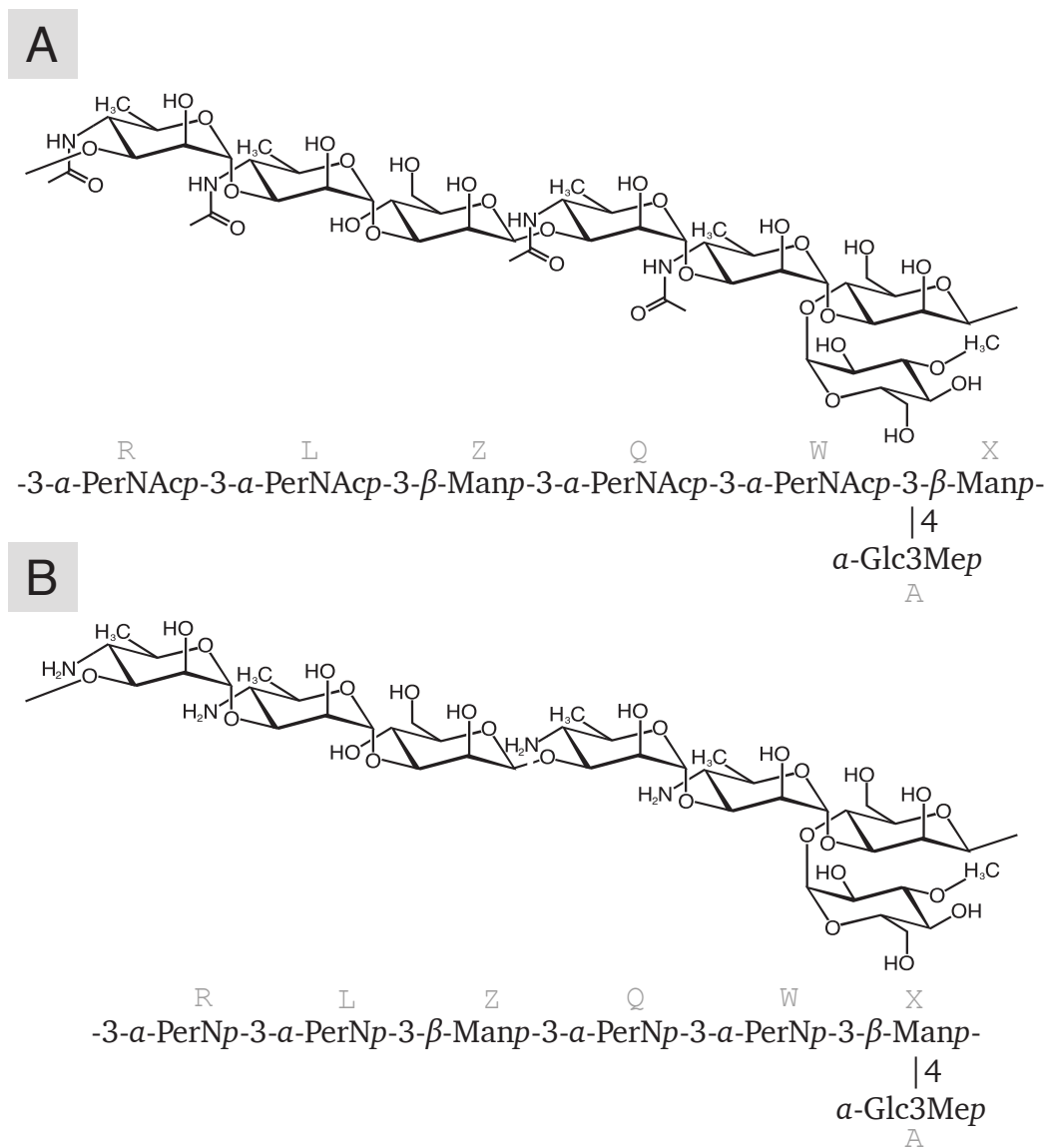


Figure 1.3: The structure of the *C. crescentus* OPS. **A.** The intact repeating unit, PS1. **B.** The deacylated product of PS1.

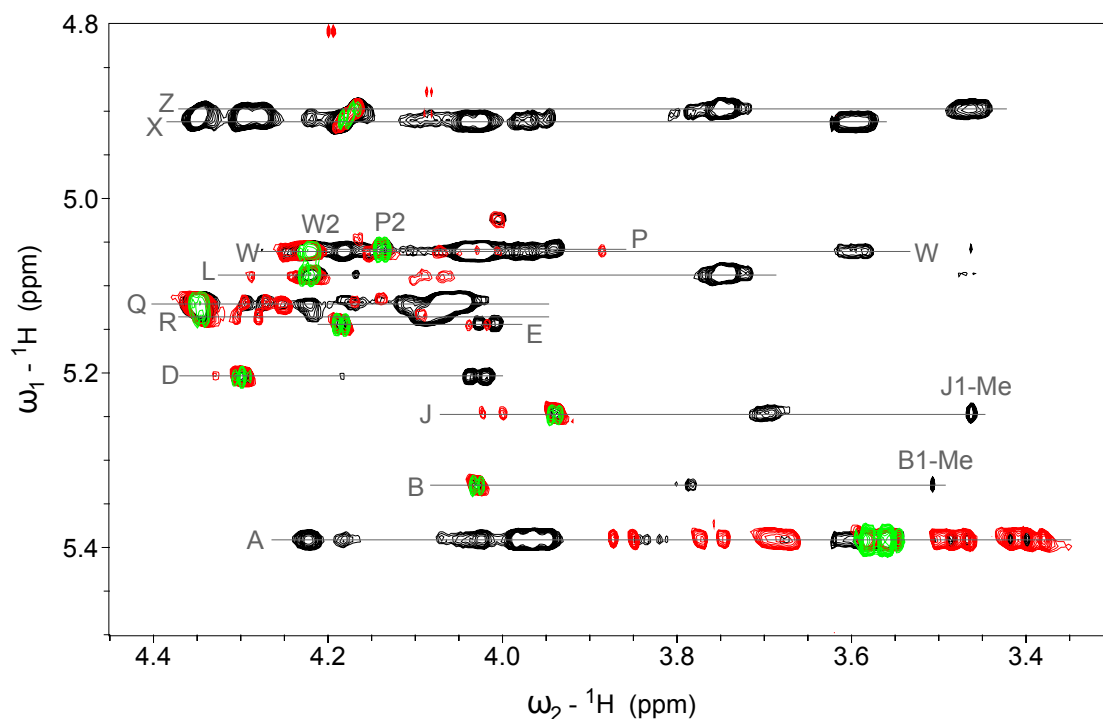


Figure 1.4: Overlap of COSY (green), TCOSY (red) and ROESY (black) correlations from anomeric protons of double oxidized deacylated *C. crescentus* PS1.

1.2.4 Minor component determination

PS and PS1 spectra contained signals of minor components, which could not be removed by chromatography, as described above. They probably represented the non-reducing ends of the major chain, PS1 (fig. 1.5). The minor components contained methylated Rha (2-O-Me-Rha residue J and 2,3-Me₂-Rha_{4N} residue B). The position of the methyl groups were found from HMBC correlations between protons of methyl groups and carbon atoms bearing OMe groups, which all were well visible and did not overlap with other signals due to their low field position. Thus, two independent structural fragments, 1 and 2, were found and are shown in fig. 1.5. Mannose residues Z' and Z'' at the non-reducing ends of these fragments were further linked to Rha_{4N} residues, indistinguishable from the Rha_{4N} of the main chain. Rha_{4N} residue D had upfield shifted C-2 and downfield shifted C-3 signals (table 1.2)), which have not been explained. It appears that its O-3 was phosphorylated, producing typical phosphorylation signal shifts and broadening of the H-3 signal, but ¹H-³¹P heteronuclear multiple-quantum correlation spectroscopy (HMQC) NMR spectrum showed no signals, possibly due to the low abundance of this residue. Possibly Rha residues inserted in the structure resembling PS1 represented the attachment point of the rhamnan (PS2) to PS1, if they were linked together.

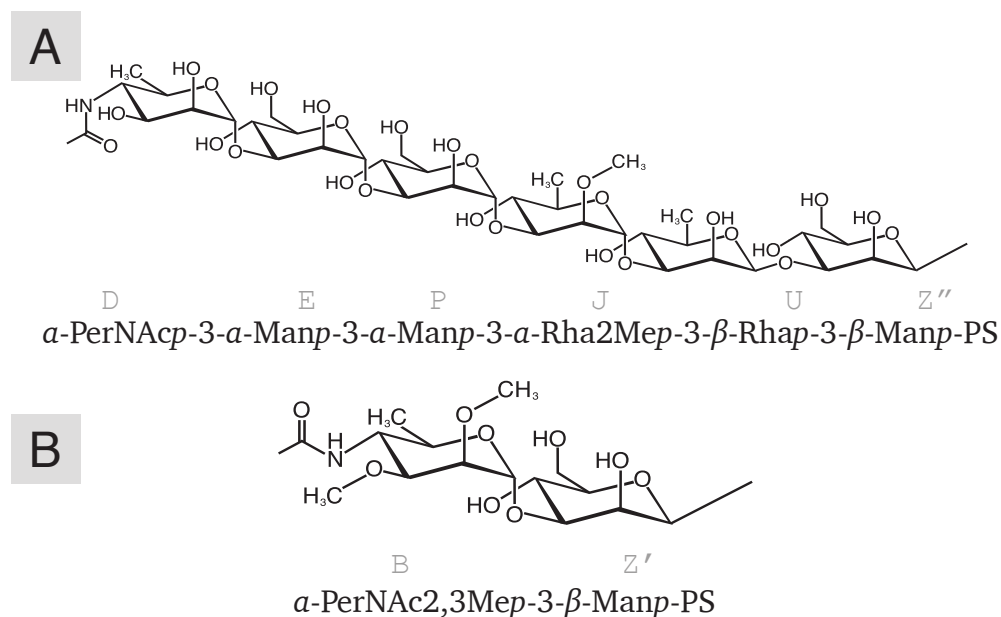


Figure 1.5: The structure of minor component, the end caps of the OPS. **A.** Fragment 1. **B.** Fragment 2.

1.2.5 Rhamnan polysaccharide determination (PS2)

Periodate oxidation of the PS produced an OS1, which was analyzed by NMR and its structure, as shown on fig. 1.6, was determined using standard 2D NMR methods. Signal assignment is shown in the table 1.3. It contained three rhamnopyranose units and 4-deoxy-1-deutero-erythritol, produced by the oxidation-reduction of 4-substituted rhamnose. Formation of this oligosaccharide could be explained by oxidation of the side chain Rha F and 4-substituted Rha G in the PS1 (letter labels for monosaccharides were given using anomeric signals in the whole PS spectra starting from low-field). The unoxidized 4-substituted residue T in the oligosaccharide originally carried side-chain Rha F at position 2. Knowing the OS1 structure the signals of a corresponding polymer (PS2) were identified in the spectra of the whole PS, and are given in the table 1.3.

1.2.6 Core oligosaccharide determination

The core oligosaccharide of the *C. crescentus* LPS isolated after AcOH hydrolysis contained one non-degraded Kdo, two LD-Hep, one DD-Hep, mannose, galactose, and glucuronic acid in pyranose form. 2D NMR analysis led to the structure shown on fig. 1.7 (NMR assignments are in table 1.4, the heteronuclear single quantum coherence (HSQC) spectrum is in fig. 1.8). The sequence followed from the observed NOE: E1:C5,C7,F5; F1:E2; G1:F3; H1:C7,E2; K1:C4; L1:K4. Correlation E1:C7 is always observed in the α -Hep-5-Kdo fragment. E1:F5 was due to the α -Man-2-Hep linkage. H1E2 indicates spatial proximity of the residues E and H, linked to the same Kdo C. All expected transglycoside correlations were observed in HMBC spectrum, together with intra-ring correlations H-1:C-3 and H-1:C-5 for all α -pyranoses.

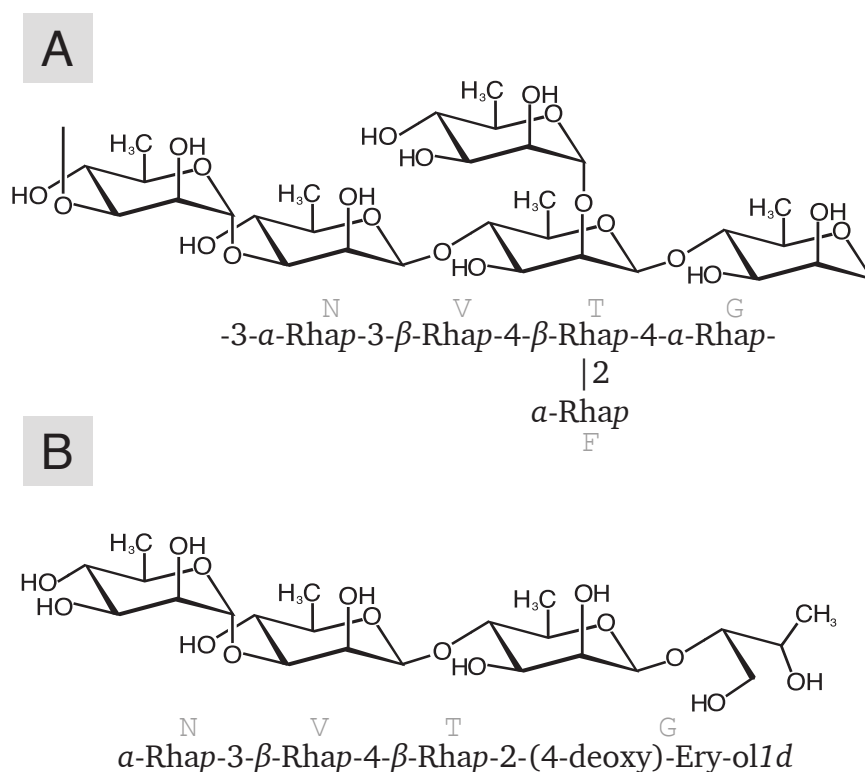


Figure 1.6: The structure of the *C. crescentus* rhamnan. **A.** the intact rhamnan, PS2. **B.** the oxidised rhamnan product, OS1.

Methylation analysis revealed terminal DD-Hep, terminal and 2-substituted LD-Hep, 3-substituted Man and terminal Gal. The structure agreed with mass spectral data, electrospray ionization (ESI) negative $[M-H]^- = 1314.9$, $[M-2H]/2^- = 656.7$, calculated exact mass Hex2Hep3HexA1Kdo1 = 1314.4 Da.

1.3 Methods

1.3.1 Bacterial strain construction and growth conditions

The strain used for the preparation of LPS was JS1025, a derivative of *C. crescentus* CB15 NA1000. The salient features are that it has an engineered amber mutation in *rsaA* leading to the loss of the S-layer and the gene CCNA_00471 has been inactivated by a partial deletion. CCNA_00471 encodes a putative GDP-L-fucose synthase.¹⁰ The knockout ($\Delta 471$) confers a deficiency in an EPS that was previously found to contain L-fucose.⁹ CCNA_00471 was disrupted in the same manner as previously in JS4038,¹¹ except the starting strain used here was JS1023.¹²

¹⁰M. E. Marks et al. *J Bacteriol*, **192**: 3678–88, 2010.

¹¹C. Farr et al. *PLoS One*, **8**: e65965, 2013.

¹²F. Amat et al. *J Bacteriol*, **192**: 5855–65, 2010.

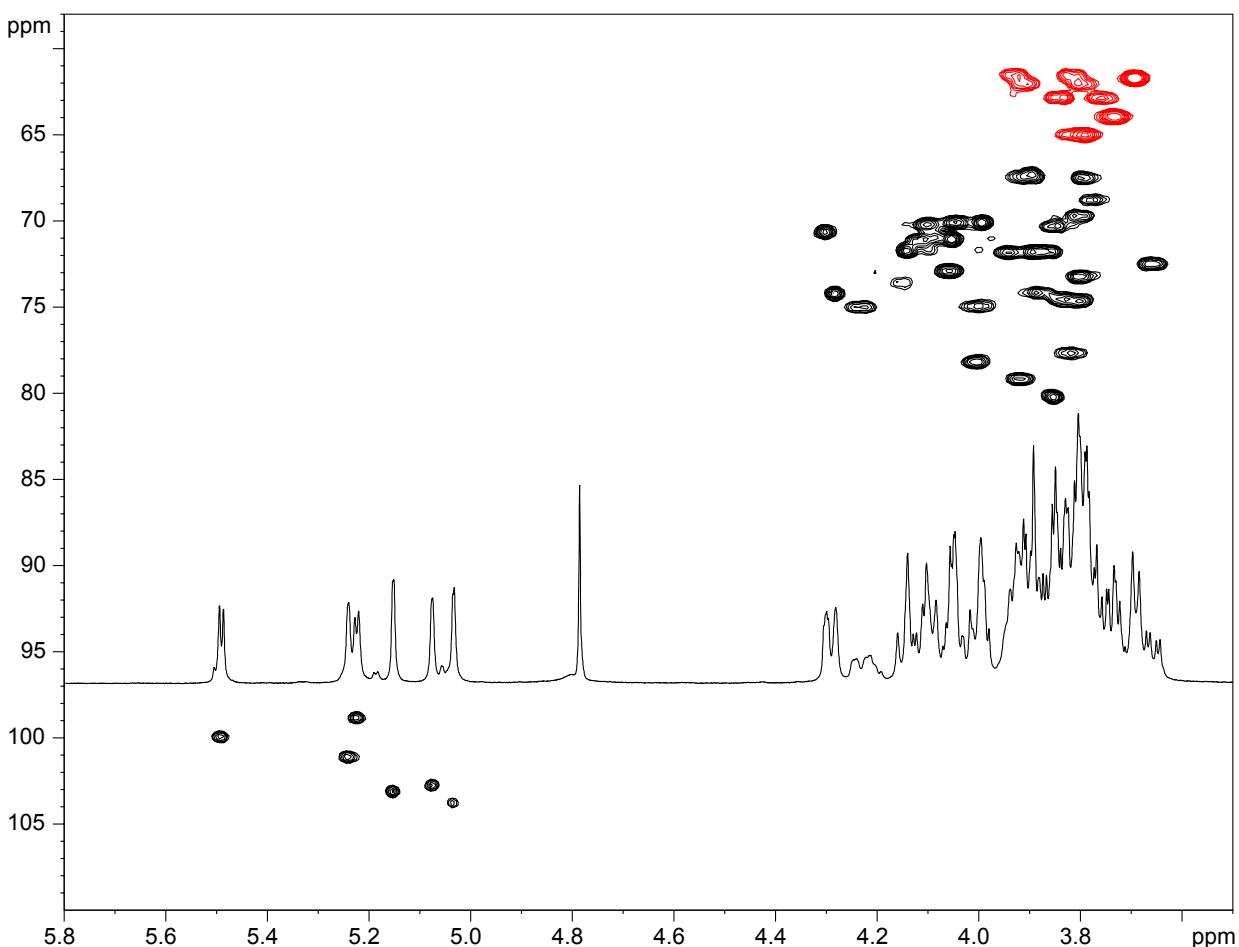


Figure 1.8: Fragment of ^1H - ^{13}C HSQC spectrum of the core.

acid (EDTA), agitated at room temperature for 10 min and then centrifuged at $15\,300 \times g$ for 15 min. The supernatant was retrieved and re-centrifuged, as before, to ensure clarity and then dialyzed against 5 mM MgCl_2 . DNase and RNase were added to final concentrations of $10 \mu\text{g ml}^{-1}$ and $100 \mu\text{g ml}^{-1}$, respectively, and incubated at 37°C for 2 h. Proteinase K was added to a final concentration of 0.3 mg ml^{-1} and the preparation was incubated at 50°C overnight. The sample was then ultracentrifuged at $184\,000 \times g$ for 3 h. Glassy pellets formed which were suspended in distilled water to 1/100 original culture volume. A Bligh-Dyer extraction was performed to reduce contaminating lipids.¹⁶

1.3.3 Bligh Dyer Extraction

A Bligh Dyer extraction was performed on all LPS preparations to reduce the presence of contaminating lipids. The extraction was performed as first published.¹⁶ In short, to one volume of aqueous LPS sample, 3.75 volumes of chloroform/methanol (1:2 v/v) was added and the sample was vortexed for 30 seconds.

Harbor Laboratory Cold Spring Harbor, NY, 1982.

¹⁶E Graham Bligh and W Justin Dyer. *Can J Biochem Physiol*, **37**: 911–917, 1959.

1.25 volumes of chloroform was added and the sample was vortexed again for 30 seconds. 1.25 volumes of water were added and the sample was vortexed a final time for 30 seconds. This mixture was then centrifuged at 15 300 x g for 10 min. After centrifugation, the mixture separated into two phases, a lower organic phase and an upper aqueous phase. The LPS partitions into the aqueous phase, while other lipids partition into the organic phase. The aqueous phase was retrieved and kept.

1.3.4 Gel electrophoresis

Discontinuous sodium dodecyl sulfate-polyacrylamide gel electrophoresis (SDS-PAGE) was performed with a 13% separating gel.¹⁷ Detection of LPS was done by periodate oxidation and silver staining as described by Zhu *et al.*¹⁸

1.3.5 NMR spectroscopy

NMR experiments were carried out on a Varian INOVA 600 MHz (¹H) spectrometer with 5 mm gradient probe at 25–50°C with acetone internal reference (2.225 ppm for ¹H and 31.45 ppm for ¹³C), using standard pulse sequences gCOSY, TCOSY (mixing time 120 ms), ROESY (mixing time 300 ms), gHSQC, and gHMBC (100 ms long range transfer delay), HMQC for ¹H-³¹P correlation, JHX set to 10 Hz. AQ time was kept at 0.8–1 sec for H-H correlations and 0.25 sec for HSQC. 256 increments were acquired for t₁ in all 2D spectra, except 512 for gCOSY.

1.3.6 LPS Chromatography

Gel chromatography was performed on a Sephadex G-15 column (1.5x60 cm) or a Bio-gel P6 column (2.5x60 cm) in pyridine-acetic acid buffer (4 ml:10 ml:1 l water), and monitored by refractive index detector (Gilson). Anion exchange chromatography was done on an Hitrap Q column (2x5 ml size, Amersham), with ultraviolet Light (UV) monitoring at 220 nm in a linear gradient of NaCl (0–1 M, 1 h) at the 3 ml min⁻¹. Fractions of 1 min were collected and additionally tested for carbohydrates, by spotting on an SiO₂ thin-layer chromatography (TLC) plate, dipping them in 5% H₂SO₄ in EtOH and heating with a heat-gun. All fractions of interest were dried in a Savant drying centrifuge and ¹H spectra were recorded for each fraction without desalting. For 2D NMR, desalting was performed on a Sephadex G15 column.

1.3.7 Monosaccharide analysis

Samples with added inositol standard were hydrolyzed with 3 M trifluoroacetic acid (TFA) at 120°C. Monosaccharides were converted to alditol acetates by conventional methods and identified by gas chromatography-mass spectroscopy (GC-MS) on a Varian Saturn 2000 instrument on a DB17 capillary column (30 m x 0.25

¹⁷Ulrich K Laemmli. *Nature*, **227**: 680–685, 1970.

¹⁸Zhong-Xin Zhu et al. *Electrophoresis*, **33**: 1220–1223, 2012.

mm ID x 0.25 μm film) with helium carrier gas, using a temperature gradient 170°C (3 min), 250°C at 5°C min⁻¹.

1.3.8 Determination of absolute configurations of monosaccharides

To the polysaccharide sample (0.2 mg) (R)-2-BuOH (0.2 ml) and acetyl chloride (0.02 ml) were added at room temperature, heated at 90°C for 2 h, dried by air stream, acetylated, analyzed by GC-MS as described above. Standards were prepared from monosaccharides of known configuration with (R)- and (S)-2-BuOH.

1.3.9 Methylation analysis

For the methylation analysis core sample (2 mg) was dephosphorylated with 50 μl of 48% HF for 20 h at +10°C, diluted with 2 ml of ethanol, precipitate collected by centrifugation, washed with 2 ml of ethanol, dried.

Methylation was performed by Ciucanu-Kerek procedure.¹⁹ 0.5 mg of the sample was dissolved in 0.5 ml of dry DMSO with heating at 100°C for 5-10 min until complete dissolution. Powdered NaOH (about 50 mg) was added and the mixture was stirred for 30 min. 0.2 ml of MeI was added and the mixture was stirred for a subsequent 30 min. The sample was then flushed with air to remove the MeI and diluted to 10 ml with water. The sample was passed through a C18 Seppak cartridge, washed with 10 ml of water, and then the methylated compound was eluted with 5 ml of methanol. The methylated product was hydrolyzed with 3 M TFA (120°C, 3h), dried, reduced with NaBD₄, and the reagent destroyed with 0.5 ml of 4 M HCl. The solution was dried under a stream of air and dried twice more with the addition of MeOH (1 ml). The sample was acetylated with 0.4 ml Ac₂O and 0.4 ml pyridine for 30 min at 100°C. It was then dried and analyzed by GC-MS.

1.3.10 Periodate oxidation

PS (10 mg) was dissolved in water (2 ml). NaIO₄ (20 mg) was added and the solution was incubated at room temperature for 24 h. Ethylene glycol (0.2 ml) and an excess NaBD₄ were added. The solution was then kept for 1 h before being treated with 0.2 ml of AcOH and desalted on a Sephadex G-15 column. The product was hydrolyzed with 2% AcOH, 2 h at 100°C, and separated on a Sephadex G-50 column to give OS1.

1.4 Discussion

The LPS of *C. crescentus* has an unusually complicated structure with two different polysaccharides, irregular substituents, and unfavourable NMR spectra. Presented data show structures of the core part, two

¹⁹Ionel Ciucanu and Francisc Kerek. *Carbohydr Res*, **131**: 209–217, 1984.

polymers, and putative terminal structures. The polysaccharides could not be separated by size exclusion or anion-exchange chromatography and are probably linked together through the same core. The core of the *C. crescentus* LPS has been studied previously and an initial assessment of its composition was made,⁸ but the complete structure had not been determined. The structure of the OPS has not been studied before. In our view the polysaccharide structure of the *C. crescentus* LPS represents one of the most complicated bacterial LPS polysaccharide structures identified so far.

The Kdo present in the LPS core structure (fig. 1.7) has the typical substitutions at O-4 and O-5 of a manno-configured sugar and a negatively charged sugar, respectively.²⁰ It also has a rarely observed third substitution at O-7 with a heptose moiety. The Kdo O-7 position is known to be occupied by a galactose moiety in the core of *Rhizobium leguminosarum* bv. *Viciae* VF39,²¹ and the secondary Kdo in the core oligosaccharide from *Acinetobacter baumannii* ATCC 19606 has an O-7 substituted with a glucosamine.²²

In the traditional model LPS occupies the outer leaflet of the outer membrane of a Gram-negative bacterium, and so (excepting the presence of cell associated EPS) is the outermost layer of the cell. For *C. crescentus*, however, LPS is the penultimate barrier below the protein S-layer. The *C. crescentus* OPS serves as the anchor for the S-layer and is likely not accessible to the environment.⁶ The carbohydrates found in the OPS are particularly hydrophobic, marked by the abundance of deoxy-sugars, acetyl groups, and methyl groups. This hydrophobicity is possibly a result of particular sugars needed for S-layer anchoring, as these carbohydrate structures likely evolved as the cognate ligands for the S-layer protein, RsaA. The distance between the S-layer and the outer membrane is about 17–19 nm.²³ It is possible the hydrophobicity aids in packing the polysaccharides between the S-layer and the LPS. Further determination of RsaA's structure should help illuminate the interaction between the S-layer and OPS.

Knowledge of the structure of *C. crescentus* OPS and LPS will facilitate the determination and characterization of their biosynthetic enzymes and mutant variants. Already, the enzymes LpxI²⁴ and GDP-L-perosamine acetylase²⁵ from *C. crescentus* have been characterized. One uncharacterized enzyme, WbqL, is necessary for proper OPS synthesis and disruption of wbqL leads to the accumulation of truncated and S-layer anchoring deficient OPS in the inner membrane and inhibits Crescentin-mediated cell curvature.²⁶ Many genes, such as wbqL, have been identified as essential for OPS synthesis⁷ but have not yet been characterized. Other genes, that must be essential for OPS synthesis, have yet to be identified or characterized, such as the O-antigen polymerase and ligase.

The subunit-based repeating nature of *C. crescentus* OPS suggests that a Wzy-dependent pathway synthesizes the polymer.²⁷ The previous study that aimed to identify genes essential for OPS did not identify many of the canonical genes in the Wzy-dependant pathway,⁷ such as the O-unit transporter, Wzx, O-antigen polymerase, Wzy; the chain-length determinate protein, Wzz; and the O-antigen ligase, WaaL.

²⁰Helmut Brade. *Endotoxin in health and disease*. New York: Marcel Dekker, 1999. xviii, 950 p.

²¹Y. Zhang, R. I. Hollingsworth, and U. B. Priefer. *Carbohydr Res*, **231**: 261–271, 1992.

²²E. V. Vinogradov et al. *Eur J Biochem*, **243**: 122–127, 1997.

²³A. Moll et al. *Mol Microbiol*, **77**: 90–107, 2010.

²⁴Louis E Metzger IV et al. *Nat Struct Mol Biol*, **19**: 1132–1138, 2012.

²⁵James B Thoden et al. *Biochemistry*, **51**: 3433–3444, 2012.

²⁶Matthew T Cabeen et al. *J Bacteriol*, **192**: 3368–3378, 2010.

²⁷C. R. H. Raetz and C. Whitfield. *Annu Rev Biochem*, **71**: 635–700, 2002.

Genes that have been annotated as putative O-antigen synthesis genes do appear in the sequenced genomes for *C. crescentus* CB15, but they have not been experimentally confirmed.

An additional aspect to this LPS is the fact that its O-antigen is of homogenous length. While other LPSS vary in size due to the number of O-antigen repeat groups, appearing as a laddering of bands by SDS-PAGE, the LPS from *C. crescentus* appears as a single band.⁶ Initial MALDI-TOF analysis of the entire LPS indicates a size of about 10.8 kDa (see fig. 1.1 on page 2). After accounting for the solved structures for the lipid A and core regions, this suggests the LPS contains approximately 5 repeats of the proposed heptameric O-antigen structure. There is not currently a known mechanism for the regulation and synthesis of a strictly homogenous length O-antigen. It is possible that this OPS is synthesized via the ATP-binding cassette (ABC)-transporter-dependent pathway²⁷ or another heretofore undiscovered mechanism. In any event it would seem that the transfer of a polysaccharide of this considerable size to the outer leaflet of the outer membrane is a remarkable feat for the bacterium.

Table 1.1: NMR data for *C. crescentus* PS1 (40°C) and deacylated PS1 (50°C). Me at 3.62/61.3 ppm.

		PS1					
		1	2	3	4	5	6
Rha4NAc R	H	4.97	3.98	4.13	3.92	3.91	1.21
	C	103.3	68.2	75.5	52.4	69.4	18.0
Rha4NAc Q	H	4.98	3.97	4.11	3.92	3.91	1.21
	C	103.3	68.2	75.5	52.4	69.4	18.0
Rha4NAc L	H	5.05	4.12	3.99	3.98	3.98	1.21
	C	103.3	70.4	78.2	53.0	69.4	18.0
Rha4NAc W	H	5.02	4.12	3.96	3.98	3.98	1.21
	C	104.0	70.4	77.8	53.0	69.4	18.0
β -Man X	H	4.74	4.09	3.98	3.90	3.54	3.80; 3.96
	C	97.8	72.1	85.4	72.1	75.8	62.6
β -Man Z	H	4.72	4.06	3.70	3.68	3.41	3.77; 3.96
	C	98.2	71.9	82.3	67.2	77.3	62.4
Glc3Me A	H	5.36	3.51	3.40	3.44	3.68	3.75; 3.85
	C	100.0	72.2	84.1	70.1	74.1	61.6
		Deacylated PS1					
Rha4N R	H	5.13	4.34	4.29	3.30	4.18	1.38
	C	103.5	67.4	75.0	53.4	67.8	18.0
Rha4N Q	H	5.11	4.34	4.29	3.30	4.18	1.38
	C	103.5	67.4	75.0	53.4	67.8	18.0
Rha4N L	H	5.08	4.22	4.06	3.11	4.09	1.35
	C	103.9	69.9	79.9	53.6	69.5	18.0
Rha4N W	H	5.06	4.22	4.06	3.11	4.09	1.35
	C	103.9	69.9	79.9	53.6	69.5	18.0
β -Man X	H	4.91	4.18	4.03	3.96	3.59	3.83; 3.96
	C	98.0	71.7	85.0	71.7	75.9	62.1
β -Man Z	H	4.90	4.18	3.75	3.75	3.46	3.83; 3.96
	C	98.0	71.7	82.0	67.0	77.4	62.1
Glc3Me A	H	5.39	3.57	3.40	3.48	3.68	3.76; 3.86
	C	100.2	72.2	84.0	70.0	74.1	61.7

Table 1.2: NMR data for the minor components of the double oxidized non-deacylated PS (50°C).
Methyl group signals: B2: 3.48/59.5; B3: 3.42/57.9; J2: 3.45/59.6 ppm (H/C)

		1	2	3	4	5	6
Rha4N2,3Me B	H	5.25	3.96	3.71	3.81	3.91	1.17
	C	100.2	76.2	78.2	53.2	69.5	18.0
α -Rha2Me J	H	5.25	3.95	4.02	3.45	3.90	1.30
	C	100.2	75.9	75.4	71.8	69.5	18.0
α -Rha4N D	H	5.14	4.27	4.20	3.95	3.97	1.23
	C	100.1	67.4	75.2	52.2	69.4	18.0
α -Man E	H	5.13	4.17	3.99	3.75	3.84	
	C	100.1	70.9	79.8	67.1	74.4	
α -Man P	H	5.05	4.14	4.00	3.85	3.96	
	C	97.6	71.0	79.5	66.9	74.0	
β -Rha U	H	4.78	4.16	3.69	3.48	3.44	1.32
	C	100.9	71.8	82.0	72.4	73.1	18.0
β -Man Z''	H	4.72	4.06	3.75	3.75	3.46	3.83; 3.96
	C	98.2	71.9	86.0	67.0	77.4	62.1
β -Man Z'	H	4.72	4.06	3.73	3.75	3.46	3.83; 3.96
	C	98.2	71.9	82.3	67.0	77.4	62.1

Table 1.3: NMR data for *C. crescentus* PS2 and its NaIO₄ oxidation product OS1 (40°C).

		1	2	3	4	5	6
α -Rha N, OS1	H	5.04	4.07	3.85	3.47	3.85	1.30
	C	103.1	71.1	71.1	72.9	69.9	17.6
α -Rha N, PS	H	5.02	4.02	3.79	3.45	3.72	1.28
	C	103.0	71.5	78.8	73.3	70.4	17.5
β -Rha T, OS1	H	4.78	4.13	3.71	3.54	3.53	1.33
	C	100.7	71.1	72.3	83.4	71.7	17.5
β -Rha T, PS	H	4.79	4.22	3.82	3.62	3.61	1.36
	C	101.7	76.7	73.5	83.4	73.2	17.5
β -Rha V, OS1	H	4.75	4.12	3.67	3.49	3.49	1.34
	C	101.1	71.4	81.3	71.9	72.9	17.5
β -Rha V, PS	H	4.77	4.13	3.66	3.66	3.50	1.35
	C	101.4	71.2	81.7	67.2	73.3	17.5
X (ox. G), OS1	H	3.69; 3.71	3.75	3.99	1.20		
	C	61.8	84.8	67.7	18.0		
α -Rha G, PS	H	5.10	4.13	3.94	3.58	3.90	1.35
	C	103.1	71.5	70.3	84.5		17.5
α -Rha F, PS	H	5.11	4.09	3.87	3.45	4.07	1.27
	C	102.4	72.1	71.3	73.3		17.5

Table 1.4: NMR data for the core oligosaccharide (25°C).

		1	2	3	4	5	6	7	8
Kdo C	H			2.05; 2.35	4.23	4.28	4.09	3.91	3.81; 3.93
	C		98.2	34.7	74.9	74.2	71.0	79.2	61.5
DLHep E	H	5.24	3.85	4.12	3.89	3.88	4.04	3.73; 3.73	
	C	101.1	80.2	71.1	67.3	74.1	70.0	63.9	
Man F	H	5.03	4.30	4.00	3.79	3.80	3.80; 3.91		
	C	103.7	70.6	78.1	67.5	74.5	62.0		
DDHep G	H	5.15	4.05	3.86	3.77	3.84	4.06	3.76; 3.84	
	C	103.1	71.0	71.8	68.7	74.5	72.9	62.9	
DLHep H	H	5.07	4.14	3.89	3.89	3.80	4.10	3.79; 3.81	
	C	102.7	73.7	71.8	67.3	73.2	70.2	64.9	
GlcA K	H	5.22	3.66	4.00	3.99	4.15			
	C	98.8	72.4	74.9	73.6				
Gal L	H	5.49	3.80	3.85	3.99	3.94	3.69; 3.69		
	C	99.9	69.7	70.3	70.0	71.8	61.6		

Bibliography

- [1] MICHAEL D JONES, CHARLES W TRAN, GUANG LI, WALTER P MAKSYMOWYCH, RONALD F ZERNICKE, and MICHAEL R DOSCHAK. In vivo microfocal computed tomography and magnetic resonance imaging evaluation of antiresorptive and antiinflammatory drugs as preventive treatments of osteoarthritis in the rat. *Arthritis & Rheumatism*, **62**: 2726–2735, 2010.
- [2] LESLIE LAMPORT. *TEX: A Document Preparation System*. 2nd ed. Addison-Wesley, 1994.
- [3] GREGOR KICZALES, JOHN LAMPING, ANURAG MENDHEKAR, CHRIS MAEDA, CRISTINA LOPES, JEAN-MARC LOINGTIER, and JOHN IRWIN. “Aspect-Oriented Programming” in: *Proceedings of the European Conference on Object-Oriented Programming (ECOOP)*. vol. 2591 Lecture Notes in Computer Science 1997. 220–242
- [4] ROBERT BRINGHURST. *The Elements of Typographic Style*. 2.5 Hartley & Marks, 2002.
- [5] JOHN SMIT, IGOR A KALTASHOV, ROBERT J COTTER, EVGENY VINOGRADOV, MALCOLM B PERRY, HIBBA HAIDER, and NILOFER QURESHI. Structure of a novel lipid A obtained from the lipopolysaccharide of *Caulobacter crescentus*. *Innate Immunity*, **14**: 25–36, 2008. (see p. 1)
- [6] STEPHEN G WALKER, D NEDRA KARUNARATNE, NEIL RAVENSCROFT, and JOHN SMIT. Characterization of mutants of *Caulobacter crescentus* defective in surface attachment of the paracrystalline surface layer. *Journal of Bacteriology*, **176**: 6312–6323, 1994. (see pp. 1, 9, 13, 14)
- [7] P. AWRAM and J. SMIT. Identification of lipopolysaccharide O antigen synthesis genes required for attachment of the S-layer of *Caulobacter crescentus*. *Microbiology*, **147**: Awram, P Smit, J Research Support, Non-U.S. Gov’t Research Support, U.S. Gov’t, Non-P.H.S. England Microbiology (Reading, England) Microbiology. 2001 Jun;147(Pt 6):1451-60., 1451–60, 2001. (see pp. 1, 13)
- [8] N. RAVENSCROFT, S. G. WALKER, G. G. DUTTON, and J. SMITH. Identification, isolation, and structural studies of the outer membrane lipopolysaccharide of *Caulobacter crescentus*. *Journal of Bacteriology*, **174**: Ravenscroft, N Walker, S G Dutton, G G Smith, J GM-39055/GM/NIGMS NIH HHS/United States Comparative Study Research Support, Non-U.S. Gov’t Research Support, U.S. Gov’t, Non-P.H.S. Research Support, U.S. Gov’t, P.H.S. United states Journal of bacteriology J Bacteriol. 1992 Dec;174(23):7595-605., 7595–605, 1992. (see pp. 1, 13)

- [9] N. RAVENSCROFT, S. G. WALKER, G. G. DUTTON, and J. SMIT. Identification, isolation, and structural studies of extracellular polysaccharides produced by *Caulobacter crescentus*. *Journal of Bacteriology*, **173**: Ravenscroft, N Walker, S G Dutton, G G Smit, J Research Support, Non-U.S. Gov't Research Support, U.S. Gov't, Non-P.H.S. United states Journal of bacteriology J Bacteriol. 1991 Sep;173(18):5677-84., 5677–84, 1991. (see pp. 1, 8)
- [10] M. E. MARKS, C. M. CASTRO-ROJAS, C. TEILING, L. DU, V. KAPATRAL, T. L. WALUNAS, and S. CROSSON. The genetic basis of laboratory adaptation in *Caulobacter crescentus*. *Journal of Bacteriology*, **192**: Marks, Melissa E Castro-Rojas, Cyd Marie Teiling, Clotilde Du, Lei Kapatral, Vinayak Walunas, Theresa L Crosson, Sean eng 1F32-GM083424/GM/NIGMS NIH HHS/ J Bacteriol. 2010 Jul;192(14):3678-88. doi: 10.1128/JB.00255-10. Epub 2010 May 14., 3678–88, 2010. DOI: 10.1128/JB.00255-10 (see p. 8)
- [11] C. FARR, J. F. NOMELLINI, E. AILON, I. SHANINA, S. SANGSARI, L. A. CAVACINI, J. SMIT, and M. S. HORWITZ. Development of an HIV-1 Microbicide Based on : Blocking Infection by High-Density Display of Virus Entry Inhibitors. *PLoS One*, **8**: Farr, Christina Nomellini, John F Ailon, Evan Shanina, Iryna Sangsari, Sassan Cavacini, Lisa A Smit, John Horwitz, Marc S Journal article PloS one PLoS One. 2013 Jun 19;8(6):e65965. Print 2013., e65965, 2013. DOI: 10.1371/journal.pone.0065965PONE-D-12-33995[pil] (see p. 8)
- [12] F. AMAT, L. R. COMOLLI, J. F. NOMELLINI, F. MOUSSAVI, K. H. DOWNING, J. SMIT, and M. HOROWITZ. Analysis of the intact surface layer of *Caulobacter crescentus* by cryo-electron tomography. *Journal of Bacteriology*, **192**: Amat, Fernando Comolli, Luis R Nomellini, John F Moussavi, Farshid Downing, Kenneth H Smit, John Horowitz, Mark Research Support, Non-U.S. Gov't United States Journal of bacteriology J Bacteriol. 2010 Nov;192(22):5855-65. doi: 10.1128/JB.00747-10. Epub 2010 Sep 10., 5855–65, 2010. DOI: JB.00747-10[pil]10.1128/JB.00747-10 (see p. 8)
- [13] J SMIT, MARK HERMODSON, and N AGABIAN. *Caulobacter crescentus* pilin. Purification, chemical characterization, and NH₂-terminal amino acid sequence of a structural protein regulated during development. *Journal of Biological Chemistry*, **256**: 3092–3097, 1981. (see p. 9)
- [14] GERMAINE COHENBAZIRE, WR SISTROM, and RY STANIER. Kinetic studies of pigment synthesis by nonsulfur purple bacteria. *Journal of Cellular and Comparative Physiology*, **49**: 25–68, 1957. (see p. 9)
- [15] TOM MANIATIS, EDWARD F FRITSCH, and JOSEPH SAMBROOK. *Molecular cloning: a laboratory manual*. vol. 545 Cold Spring Harbor Laboratory Cold Spring Harbor, NY, 1982. (see p. 9)
- [16] E GRAHAM BLIGH and W JUSTIN DYER. A rapid method of total lipid extraction and purification. *Canadian journal of biochemistry and physiology*, **37**: 911–917, 1959. (see p. 10)
- [17] ULRICH K LAEMMLI. Cleavage of structural proteins during the assembly of the head of bacteriophage T4. *nature*, **227**: 680–685, 1970. (see p. 11)

- [18] ZHONG-XIN ZHU, WEI-TAO CONG, MAO-WEI NI, XI WANG, WEI-DE MA, WEI-JIAN YE, LI-TAI JIN, and XIAO-KUN LI. An improved silver stain for the visualization of lipopolysaccharides on polyacrylamide gels. *Electrophoresis*, **33**: 1220–1223, 2012. DOI: 10.1002/elps.201100492 (see p. 11)
- [19] IONEL CIUCANU and FRANCISC KEREK. A simple and rapid method for the permethylation of carbohydrates. *Carbohydrate Research*, **131**: 209–217, 1984. (see p. 12)
- [20] HELMUT BRADE. *Endotoxin in health and disease*. New York: Marcel Dekker, 1999. xviii, 950 p. (see p. 13)
- [21] Y. ZHANG, R. I. HOLLINGSWORTH, and U. B. PRIEFER. Characterization of Structural Defects in the Lipopolysaccharides of Symbiotically Impaired Rhizobium-Leguminosarum Biovar Viciae Vf-39 Mutants. *Carbohydrate Research*, **231**: Jf925 Times Cited:26 Cited References Count:19, 261–271, 1992. DOI: Doi10.1016/0008-6215(92)84024-M (see p. 13)
- [22] E. V. VINOGRADOV, K. BOCK, B. O. PETERSEN, O. HOLST, and H. BRADE. The structure of the carbohydrate backbone of the lipopolysaccharide from Acinetobacter strain ATCC 17905. *European Journal of Biochemistry*, **243**: We132 Times Cited:44 Cited References Count:28, 122–127, 1997. DOI: Doi10.1111/J.1432-1033.1997.0122a.X (see p. 13)
- [23] A. MOLL, S. SCHLIMPERT, A. BRIEGEL, G. J. JENSEN, and M. THANBICHLER. DipM, a new factor required for peptidoglycan remodelling during cell division in Caulobacter crescentus. *Molecular Microbiology*, **77**: 615WG Times Cited:21 Cited References Count:89, 90–107, 2010. DOI: Doi10.1111/J.1365-2958.2010.07224.X (see p. 13)
- [24] LOUIS E METZGER IV, JOHN K LEE, JANET S FINER-MOORE, CHRISTIAN RH RAETZ, and ROBERT M STROUD. LpxI structures reveal how a lipid A precursor is synthesized. *Nature structural molecular biology*, **19**: 1132–1138, 2012. (see p. 13)
- [25] JAMES B THODEN, LAURIE A REINHARDT, PAUL D COOK, PATRICK MENDEN, WW CLELAND, and HAZEL M HOLDEN. Catalytic Mechanism of Perosamine N-Acetyltransferase Revealed by High-Resolution X-ray Crystallographic Studies and Kinetic Analyses. *Biochemistry*, **51**: 3433–3444, 2012. (see p. 13)
- [26] MATTHEW T CABEEN, MICHELLE A MUROLO, ARIANE BRIEGEL, N KHAI BUI, WALDEMAR VOLLMER, NORA AUSMEES, GRANT J JENSEN, and CHRISTINE JACOBS-WAGNER. Mutations in the lipopolysaccharide biosynthesis pathway interfere with crescentin-mediated cell curvature in Caulobacter crescentus. *Journal of Bacteriology*, **192**: 3368–3378, 2010. (see p. 13)
- [27] C. R. H. RAETZ and C. WHITFIELD. Lipopolysaccharide endotoxins. *Annual Review of Biochemistry*, **71**: 582MJ Times Cited:1425 Cited References Count:387, 635–700, 2002. DOI: Doi10.1146/Annurev.Biochem.71.110601.135414 (see pp. 13, 14)

Appendix A

Supporting Materials

This would be any supporting material not central to the dissertation. For example:

- Authorizations from Research Ethics Boards for the various experiments conducted during the course of research.
- Copies of questionnaires and survey instruments.